

The Influence of Potential and Temperature on the Kinetics of Oxygen Reduction on Alloy 22 in Neutral Chloride Solutions.

D. Zagidulin, P. Jakupi, B. Sherar, J.J. Noël, D.W. Shoesmith.

Department of Chemistry, University of Western Ontario, London, Ontario N6A 5B7,
Canada

The passive film on Alloy 22, and its influence on the kinetics of oxygen reduction, has been studied in neutral 5 mol dm⁻³ NaCl at temperatures from 30°C to 90°C using Electrochemical Impedance Spectroscopy, X-Ray Photoelectron Spectroscopy and Cyclic Voltammetry. The impedance is very dependent on potential but only slightly dependent on temperature. Passivity is maximized, and oxygen reduction most suppressed, over the potential range -0.2 V to 0.2 V. At higher potentials the passive film resistance decreases markedly, leading to catalysis of oxygen reduction in the range 40°C to 60°C. At higher temperatures catalysis is lost.

Introduction

Alloy-22 is the candidate for the reference material for the outer corrosion barrier on waste packages to be placed in the proposed nuclear waste repository at Yucca Mountain, NV, USA (1-4). Groundwaters entering this site will be dilute, close to neutral pH, and non-corrosive (5). However, seepage water contacting the waste package could evaporatively concentrate to produce a concentrated, corrosive environment (5-8) potentially leading to crevice corrosion over the required long-term containment period.

With this application in mind, intergranular corrosion (9, 10), localized corrosion (5, 11-16), stress corrosion cracking (17-20), and general passive corrosion studies have been undertaken (21-28). In addition, surface analytical studies have been performed, including X-Ray Photoelectron Spectroscopy (XPS) and Time of Flight Secondary Ion Mass Spectroscopy (ToF SIMS) (24, 29), Atomic Force Microscopy (AFM) (28, 30), and Electron Backscatter Diffraction (EBSD) (28). Attempts have also been made to model various aspects of corrosion in the repository (13, 17, 31, 32).

Persuasive arguments can be made that Alloy 22 will not sustain significant corrosion damage under Yucca Mountain conditions (5, 33-35), but experimental evidence is meagre. The development of localised corrosion models requires a knowledge of the mechanism and kinetics of the cathodic reaction (O₂ reduction) (ORR). This reaction has been studied on noble metals, carbon, and electrically conductive oxides (36-40), but many details remain unresolved (41) and it is clear that the kinetics are surface and material specific (41).

Here, we describe our studies on the ORR on Alloy 22 under conditions approaching those anticipated in Yucca Mountain. The primary goal is to determine the influence of the passive film, and its variation with potential (E) and temperature (T).

Experimental

The composition of the alloy is given in Table I. Cylindrical samples with a geometrical surface area of 0.785 cm^2 were machined from plate materials (Haynes International, Kokomo, Indiana (USA)). Electrodes were ultrasonically cleaned in methanol and ultrapure water ($18.2 \text{ M}\Omega \text{ cm}^{-1}$), and then wet polished to a 1200 grit finish ($0.8 \mu\text{m}$), and rinsed with ultrapure water. All experiments were carried out in a 5.0 mol dm^{-3} NaCl solution, prepared from reagent grade chemicals and ultrapure water and either deaerated with (Ar) or saturated with oxygen for 60 min prior to starting an experiment. Purging was continued throughout each experiment.

The cell temperature was control using a water-circulating thermostatic bath (Fisher Scientific bath, model ISOTERM 3016H). A Pt counter electrode and Ag/AgCl (sat'd KCl) reference electrode were used. Electrochemical measurements were made using a Solartron 1287 potentiostat and Solartron 1255B frequency response analyzer.

To avoid erratic results due to the presence of air a formed oxide (42, 43) the time between sample preparation and solution immersion was minimized, and electrodes were cathodically cleaned at -1 V for 60 minutes. The cathodic currents recorded for water reduction at -1 V confirmed that this procedure created a surface with reproducible properties.

In EIS and XPS experiments the potential (E) was stepped to a constant value in the range -0.8 V to 1 V for 120 minutes. The electrode was then either removed for XPS analysis or an EIS spectrum (from 10^5 to 10^{-3} Hz) recorded and E increased to the next value in the sequence. The current (i)-time (t) behaviour was recorded at each potential. CorrWare®, CorrView®, ZPlot® and ZView® software packages from Scribner Associates Inc. were used to control EIS experiments and analyse EIS spectra.

In ORR studies, oxides were grown at a value of E in the range -0.6 V to 0.6 V . The potential was then scanned from E to -1 V to determine the influence of the oxide film on ORR kinetics, and then from -1 V back to E to observe whether cathodic reduction of the oxide film led to changes in ORR kinetics. An electrode rotation rate of 23.5 Hz eliminated diffusive effects.

XPS analyses were performed using a Kratos Axis Ultra XPS. A monochromatic AlK α X-ray source was used for all samples. All spectra were analysed using the CasaXPS software (44). Peak shifts due to charging were corrected for by adjusting the C 1s peak to 284.8 eV . A Shirley-type background correction was used to remove most of the extrinsic loss structure (45). All binding energies reported have an error of 0.35 eV . The Cr 2p high resolution spectra were fitted with fixed parameters according to Biesinger M.C. *et. al.* (46). Ni 2p spectra were fitted using parameters obtained from (47).

Results and Discussions.

X-Ray Photoelectron Spectroscopy.

XPS spectra were obtained for the surfaces oxidized at $-0.4 \text{ V} \leq E \leq 0.6 \text{ V}$ at T from 30°C to 70°C . All the alloy components were observed in survey spectra, but the W 4f

signal is very weak and not used in analyses. Figure 1 shows the influence of E and T on oxide composition. The relative concentrations of Ni and Cr show a significant dependence on both E and T compared to Mo. The Cr content increases while that of Ni decreases with increasing E, probably due to preferential release of Ni to solution and the accumulation of Cr in a thickening oxide/hydroxide (48).

Deconvolution of high resolution XPS spectra shows the presence of metallic Cr, Cr(III) oxide (Cr_2O_3) and the dominant hydroxide ($\text{Cr}(\text{OH})_3$), Figure 2. The hydroxide may have formed during the cathodic pre-treatment (48). For all three T, the relative concentration of $\text{Cr}(\text{OH})_3$ varies little with E up to 0.2 V, but increases measurably for 0.4 V and 0.6 V, accompanied by a decrease in the relative amount of Cr, consistent with an increase in film thickness for $E > 0.2$ V. A significant dependence of Cr_2O_3 relative concentration on E is observed, with a maximum at 0.2 V for 30°C and 50°C, but at more negative E at 70°C.

Ni is present as Ni metal, Ni(II) oxide (NiO) and hydroxide ($\text{Ni}(\text{OH})_2$), Figure 3, with the relative concentrations of Ni and Ni(II) oxide decreasing for $E \geq 0.2$ V, consistent with film thickening of the oxide/hydroxide with E. The $\text{Ni}(\text{OH})_2$ and $\text{Cr}(\text{OH})_3$ behaviours differ with E and T. For 30°C and 50°C, $\text{Ni}(\text{OH})_2$ increases for $E \geq 0.2$ V, but at 70°C the $\text{Ni}(\text{OH})_2$ relative concentration is only detectable at 0.2 V and 0.4 V. At 0.6 V at 70°C no Ni is observed in the analyzed layer (~ 5 nm), an indication of its predominant dissolution for these conditions.

Electrochemical Impedance Spectroscopy.

EIS spectra were fitted using a series combination of two time constants (τ). The higher frequency τ is tentatively assigned to a charge transfer process at either the alloy/oxide or oxide/solution interface and the lower frequency τ to defect migration in the oxide film. From these fits a value of the total resistance of the alloy/solution interface, the polarization resistance (R_p), is obtained. A more complete analysis of our impedance data will be published elsewhere.

Figure 4 shows R_p as a function of E and T. For $E < -0.8$ V the predominant reaction is water reduction. Any film present is very defective, with a high concentration of charge carriers. For $E = -0.6$ V, the impedance increases by 2 to 3 orders of magnitude consistent with the growth of a more insulating surface oxide. Unfortunately, XPS data for $E < -0.4$ V are unreliable due to surface oxidation during transfer of the specimen to the XPS chamber. At $E = -0.4$ V an increase in T (30°C to 70°C) leads to an increase in Cr content, primarily at the expense of the Ni content, Figure 1 and Figure 2.

For $-0.6 \text{ V} \leq E \leq 0 \text{ V}$, R_p increases steadily with no clearly apparent T dependence, due to a decrease in defect concentration in the oxide (49). R_p achieves a T independent maximum between -0.2 V and 0.2 V , Figure 4, when the Cr_2O_3 content reaches a maximum fraction, is consistent with the presence of a Cr_2O_3 insulating barrier layer.

For $E > 0.2 \text{ V}$, R_p decreases rapidly with increasing E. For $T \geq 60^\circ\text{C}$, R_p does not change over the range 0.4 V to 0.6 V, but then falls rapidly as the transpassive region is approached ($E \geq 0.8 \text{ V}$). For $T > 60^\circ\text{C}$, this arrest in the decrease in R_p with T between 0.4 V and 0.6 V is not observed, and R_p falls to values 1 to 2 orders of magnitude less than at the lower temperatures.

The Cr content of the film increases for $E \geq 0.2$ V while that of Ni decreases (Figure 1). The decrease in relative importance of metal and metal oxide, compared to metal hydroxide, signals indicates a thickening of the oxide/hydroxide layer, suggesting defects injection into the Cr_2O_3 barrier layer, leading to defect transport and film thickening, and accounting for the decrease in R_p .

Cyclic voltammetry.

Figure 5 shows voltammograms recorded after oxidation at different E and T in O_2 -saturated solution. On the negative-going scan, the influence of the oxide film on ORR kinetics is observed. On the reverse, positive-going scan, the influence on the ORR of cathodic reduction of the oxide film is determined.

For pre-oxidation at -0.4 V and -0.6 V the ORR wave is not strongly affected by the pre-oxidation potential; i.e., only a slight revival of the current is observed on the reverse scan compared to the forward scan. The behaviour is relatively insensitive to T, and consistent with EIS observations showing the oxide present at these potentials is highly defective.

Pre-oxidation at -0.2 V to +0.2 V (R_p maximum, Figure 4) led to strong suppression and little renewal of the ORR, especially at 0 V. Also, while the current can be readily revived at 30°C for -0.2 V and 0.2 V, it is less readily revived at 50°C, and not at all at 70°C, consistent with the increased Cr content of the oxide in this E region as T is increased, Figure 1. This would imply that the Cr content of the barrier layer is the primary determinant of both ORR kinetics and the redox reversibility of the oxide film.

After pre-oxidation at 0.4 V and 0.6 V (where R_p decreases, Figure 4), the ORR is very dependent on T. This is not surprising since R_p varies by two orders of magnitude for T below and above ~60°C. At 30°C the ORR is suppressed on the forward scan, consistent with high R_p values, but revived on the reverse scan, indicating the oxide is readily reducible. At 50°C, after pre-oxidation at 0.6 V, the current is not suppressed on the forward scan and is lower on the reverse scan, suggesting that as E is increased from 0.4 V to 0.6 V at 50°C the injection of defects into the film leads to the formation of catalytic states for the ORR which are lost by reduction at negative potentials. A possibility is that these catalytic states are higher oxidation states of the metal cations in the oxide. At 70°C, the ORR current is suppressed and not revived at both pre-oxidation potentials. That the ORR is enhanced by oxidation at 50°C but completely suppressed at 70°C is surprising, since R_p at 70°C is two orders of magnitude lower than at 50°C. This suggests that whether or not the ORR is observed at these temperatures is not only dependent on R_p , but also on the chemical state of the interface. A more detailed investigation of the chemistry of the surface is underway.

Summary and Conclusions

The influences of potential and temperature on the kinetics of the ORR have been studied in neutral 5.0 mol.dm⁻³ NaCl solution.

- EIS studies show that the overall resistance of the alloy/solution interface increases by ~3 orders of magnitude between -0.8 V and -0.6 V due to the growth of a passive oxide on the alloy surface.

- Over the potential range from -0.6 V to 0.2 V, the interfacial resistance increases further by up to one order of magnitude.
- For potentials up to 0.2 V, the temperature dependence of the oxide film resistance is minor.
- XPS analyses show that Cr is the dominant surface element and primarily present as $\text{Cr}(\text{OH})_3$. A peak in the Cr_2O_3 content of the oxide at 0.2 V supports the conclusion that passivity can be attributed to a Cr(III) oxide barrier layer at the alloy/film interface.
- The Cr content of the surface increases with temperature up to 70°C , which accounts for the maintenance of high oxide resistances up to this temperature.
- For potentials > 0.2 V, the oxide resistance decreases significantly with potential and XPS analyses indicate a thickening of the oxide and an increase in its $\text{Cr}(\text{OH})_3$ content. This is consistent with the injection of defects leading to a degradation of the barrier layer.
- The kinetics of the ORR are influenced significantly by the pre-oxidation potential. For pre-oxidation up to ~ 0.2 V the kinetics are only subtly influenced by potential.
- For pre-oxidation in the range -0.2 V to 0.2 V, the ORR can be totally suppressed and is difficult to revive since the oxide film is resistant to cathodic reduction.
- For $E > 0.2$ V ORR kinetics are dependent on both oxide resistance and composition, especially at intermediate temperatures ($\sim 50^\circ\text{C}$). Destruction of the barrier layer in this potential region appears to allow the formation of catalytic states for the ORR at intermediate temperatures. Their absence at higher temperatures may be due to their dissolution.

Acknowledgements.

We are grateful to Surface Science Western for surface analyses. Support by the Science & Technology Program of the Office of the Chief Scientist (OCS), Office of Civilian Radioactive Waste Management (OCRWM), U.S. Department of Energy (DOE), is gratefully acknowledged. The work was performed under the Corrosion and Materials Performance Cooperative, DOE Cooperative Agreement Number: DE-FC28-04RW12252. The views, opinions, findings, and conclusions or recommendations of authors expressed herein do not necessarily state or reflect those of the DOE/OCRWM/OCS.

Table I Nominal chemical composition of Alloy 22 (wt. %) (50).

Ni	Cr	Mo	W	Co	Fe	Si	Mn	C	V
56(as balance)	22	13	3	<2.5	3	<0.08	<0.5	<0.01	<0.35

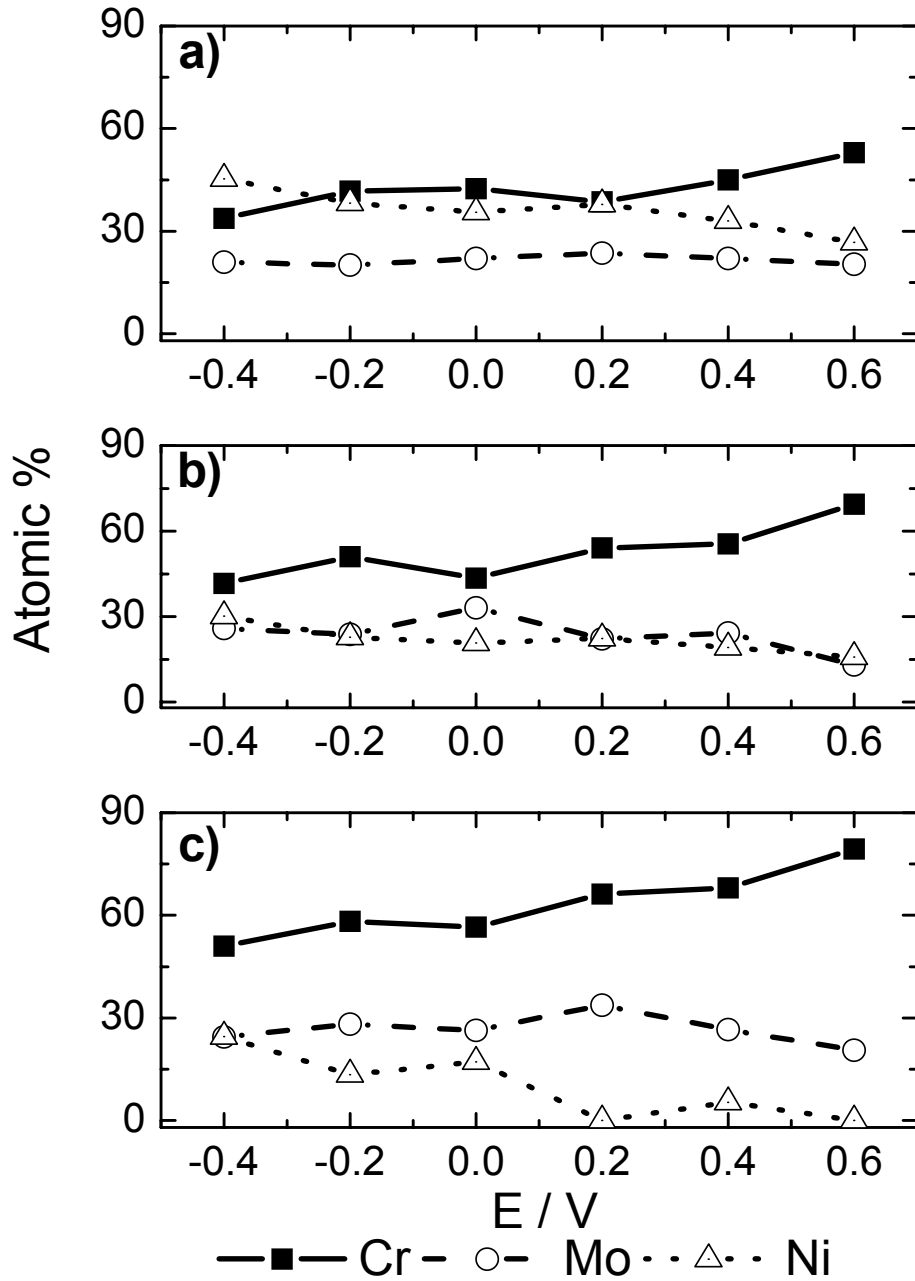


Figure 1. Relative elemental composition of the alloy surface as a function of pre-oxidation potential at different temperatures – a) 30°C; b) 50°C; c) 70°C .

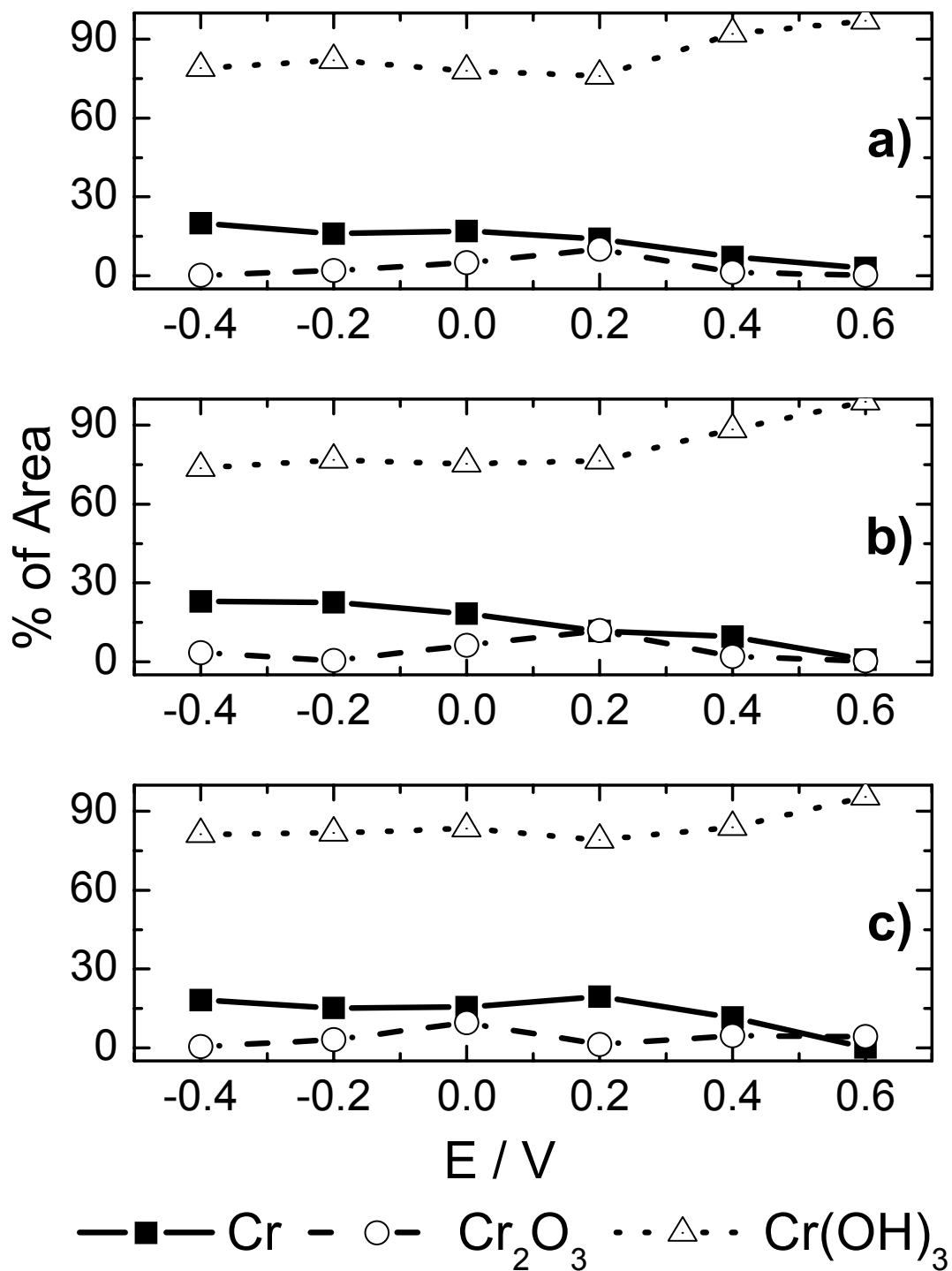


Figure 2. Relative concentrations of Cr, Cr₂O₃ and Cr(OH)₃ in the alloy surface as a function of pre-oxidation potential for different temperatures: 30°C (a); 50°C (b) and 70°C (c).

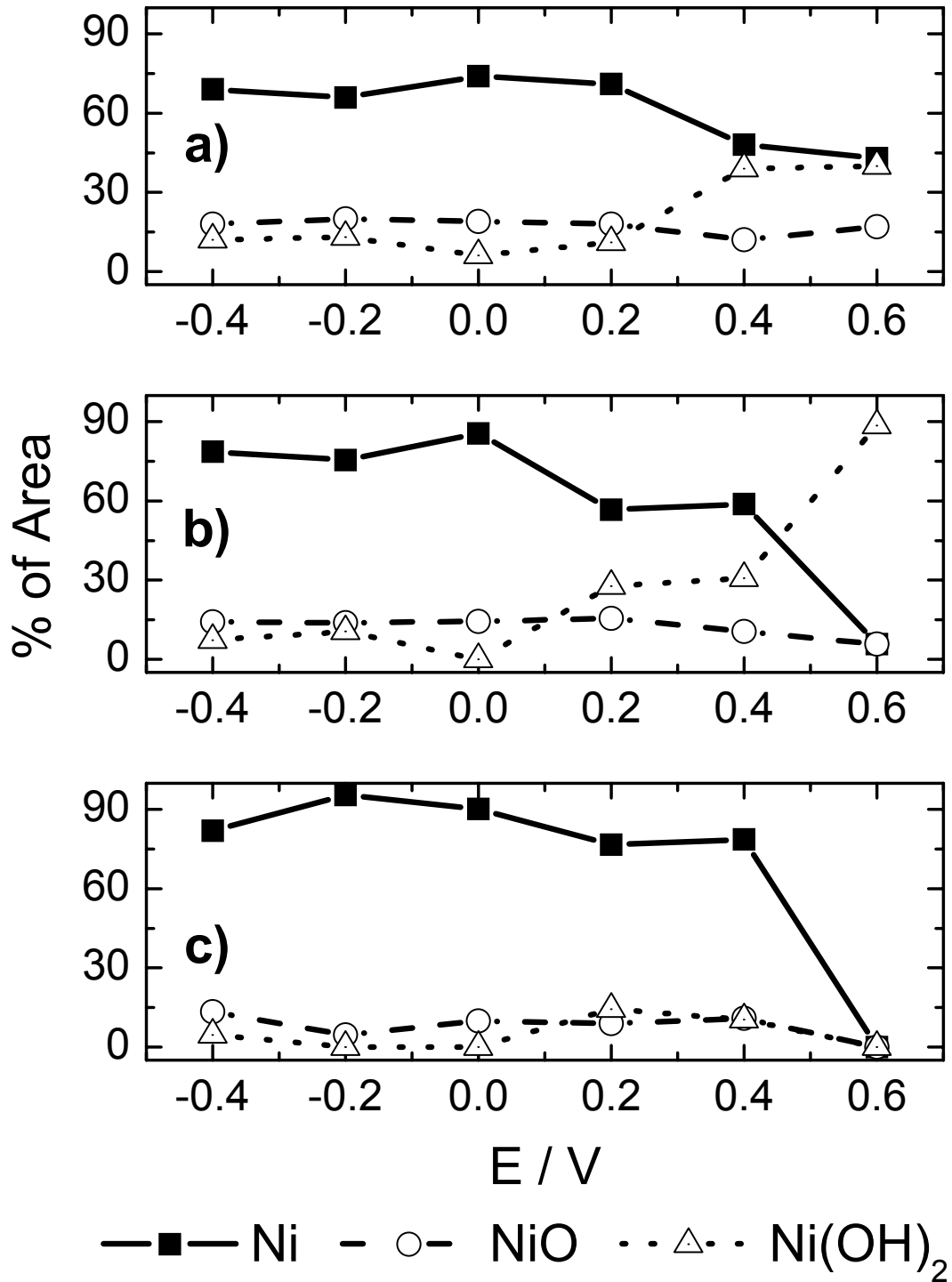


Figure 3. Relative concentrations of Ni, NiO and Ni(OH)₂ in the alloy surface as a function of pre-oxidation potential for different temperatures: 30°C (a); 50°C (b) and 70°C (c).

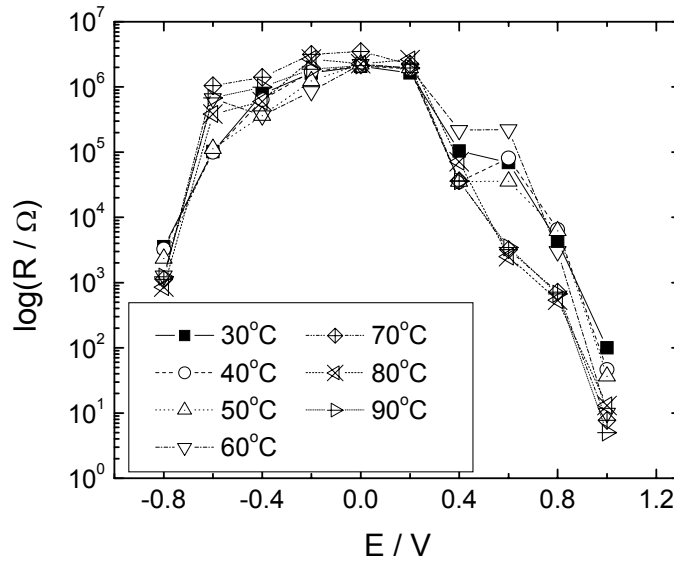


Figure 4. Polarization resistance (R_p) as a function of pre-oxidation potential and temperature

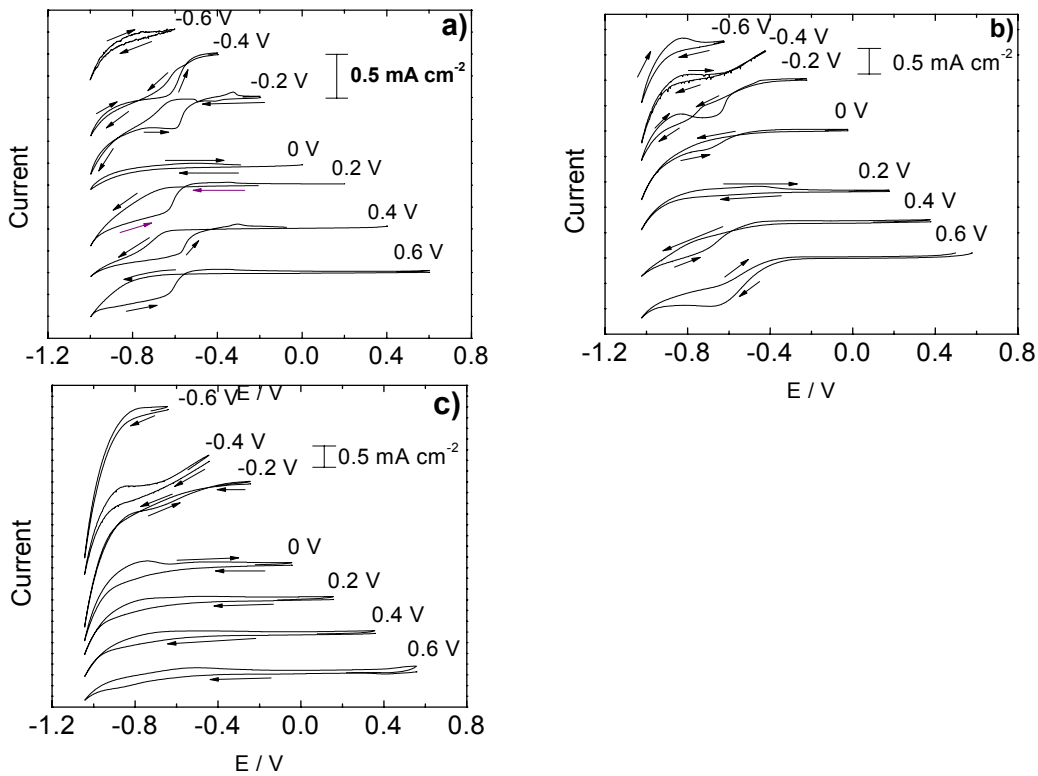


Figure 5. Cyclic voltammograms recorded on pre-oxidized Alloy 22 surfaces in oxygen-saturated solutions at 30°C (a), 50°C (b) and 70°C (c). Arrows show the direction of the potential scan.

References

1. U.S. Department of Energy, Office of Civilian Radioactive Waste Management Report M&O, ANL-EBS-MD-000003 REV. 0 (2000).
2. U.S. Department of Energy, Office of Civilian Radioactive Waste Management Report M&O 2002, Peer review of the Waste Package Material Performance, Final report, February 28 (2002).
3. U.S. Department of Energy, Office of Civilian Radioactive Waste Management Report 2003, DE-AC28-01RW1201 (2003).
4. U.S. Department of Energy, Office of Civilian Radioactive Waste Management Report M&O 2000, ANL-EBS-MD-000001 REV. 0 (2000).
5. G. M. Gordon, *Corrosion*, **58**, 811 (2002).
6. C. Steedel, in *Nuclear Waste Technical Review Board meeting*, Washington, DC (2004).
7. J. I. Driver, in *The Geochemistry of Natural Waters. Surface and Groundwater Environments.*, Prentice Hall, NJ (1997).
8. D. W. Shoesmith, *Corrosion*, **60**, 703 (2006).
9. K. S. Raja, S. A. Namjoshi, and D. A. Jones, *Metallurgical and Materials Transactions A-Physical Metallurgy and Materials Science*, **36A**, 1107 (2005).
10. D. D. Gorhe, K. S. Raja, S. A. Namjoshi, V. Radmilovic, A. Tolly, and D. A. Jones, *Metallurgical and Materials Transactions A-Physical Metallurgy and Materials Science*, **36A**, 1153 (2005).
11. D. S. Dunn, L. Yang, C. Wu, and G. A. Cragolino, in *Scientific Basis for Nuclear Waste Management XXVIII/2004*, p. 33, Materials Research Society Symposium Proceedings (2004).
12. S. D. Day, M. T. Whalen, K. J. King, G. A. Hust, L. L. Wong, J. C. Estill, and R. B. Rebak, *Corrosion*, **60**, 804 (2004).
13. D. D. Macdonald, G. Engelhardt, P. Jayaweera, N. Priyantha, and A. Davydov, *European Federation of Corrosion Publications*, **36**, 103 (2003).
14. B. A. Kehler, G. O. Ilevbare, and J. R. Scully, *Corrosion*, **57**, 1042 (2001).
15. K. J. Evans, A. Yilmaz, S. D. Day, L. L. Wong, J. C. Estill, and R. B. Rebak, *JOM*, **57**, 56 (2005).
16. D. S. Dunn, Y. M. Pan, K. T. Chiang, L. Yang, G. A. Cragolino, and X. He, *JOM*, **57**, 49 (2005).
17. P. L. Andresen, G. M. Gordon, and S. C. Lu, *JOM*, **57**, 27 (2005).
18. P. L. Andresen, L. M. Young, G. M. Catlin, P. W. Emigh, and G. M. Gordon, *Metallurgical and Materials Transactions A-Physical Metallurgy and Materials Science*, **36A**, 1187 (2005).
19. G. A. Cragolino, D. S. Dunn, and Y. M. Pan, in *Scientific Basis for Nuclear Waste Management XXVII/2004*, p. 435, Materials Research Society Symposium Proceedings (2004).
20. Y. M. Pan, D. S. Dunn, L. Yang, and G. A. Cragolino, in *Scientific Basis for Nuclear Waste Management XXVI/2002*, p. 743, Materials Research Society Symposium Proceedings (2002).

21. A. C. Lloyd, R. J. Schuler, J. J. Noël, D. W. Shoesmith, and F. King, in *Scientific Basis for Nuclear Waste Management XXVIII/2004*, p. 3, Materials Research Society Symposium Proceedings (2004).
22. A. C. Lloyd, D. W. Shoesmith, J. J. Noël, and N. S. McIntyre, in *Environmental Degradation of Materials and Corrosion Control in Metals/2003*, p. 31, Proceedings of the International Symposium on Environmental Degradation of Materials and Corrosion Control in Metals, Vancouver, BC, Canada (2003).
23. K. J. Evans, A. Yilmaz, S. D. Day, L. L. Wong, J. C. Estill, and R. B. Rebak, *JOM*, **57**, 56 (2005).
24. A. C. Lloyd, D. W. Shoesmith, N. S. McIntyre, and J. J. Noël, *J Electrochem Soc*, **150**, B120 (2003).
25. A. C. Lloyd, J. J. Noël, N. S. McIntyre, and D. W. Shoesmith, *JOM*, **57**, 31 (2005).
26. J. R. Hayes, A. Szmodis, K. L. Anderson, and C. A. Orme, Paper No. 04697, *Corrosion 2004*, NACE International (2004).
27. T. Lian, J. C. Estill, G. A. Hust, and R. B. Rebak, Paper No. 03694, *Corrosion 2003*, NACE International (2003).
28. J. J. Gray, B. S. El Dasher, and C. A. Orme, *Surf Sci*, **600**, 2488 (2006).
29. A. C. Lloyd, J. J. Noël, S. McIntyre, and D. W. Shoesmith, *Electrochim Acta*, **49**, 3015 (2004).
30. A. W. Szmodis, K. L. Anderson, J. C. Farmer, T. Lian, and C. A. Orme, Paper No. 03692, *Corrosion 2003*, NACE Internationals (2003).
31. Z. Qin and D. W. Shoesmith, in *Scientific Basis for Nuclear Waste Management XXVIII/2004*, p. 11, Materials Research Society Symposium Proceedings (2004).
32. D. S. Dunn, O. Pensado, C. S. Brossia, G. A. Cragolino, N. Sridhar, and T. M. Ahn, *European Federation of Corrosion Publications*, **36**, 208 (2003).
33. D. W. Shoesmith, in *Scientific Basis for Nuclear Waste Management XXV/2002*, p. 71, Materials Research Society Symposium Proceedings (2002).
34. J. Payer, in *Nuclear Waste Technical Review Board meeting/2004*, (2004).
35. M. Apted, F. King, D. Langmuir, R. Arthur, and J. Kessler, *JOM*, **57**, 43 (2005).
36. N. M. Markovic, R. R. Adzic, and V. B. Vesovic, *J Electroanal Chem*, **165**, 121 (1984).
37. W. H. Hocking, J. S. Betteridge, and D. W. Shoesmith, *J Electroanal Chem*, **379**, 339 (1994).
38. Matsumoto Y., *Bull Chem Soc Jpn*, **51**, 1927 (1978).
39. N. A. Anastasijevic, Z. M. Dimitrijevic, and R. R. Adzic, *J Electroanal Chem*, **199**, 351 (1986).
40. R. R. Adzic, N. M. Markovic, and V. B. Vesovic, *J Electroanal Chem*, **165**, 105 (1984).
41. E. J. M. O'Sullivan and E. J. Calvo, *Compr Chem Kinet*, **27**, 247 (1987).
42. J. G. Stoecker, O. W. Siebert, and P. E. Morris, *Materials Performance*, **22**, 13 (1983).
43. P. E. Morris and R. C. Scarberry, *Corrosion*, **26**, 169 (1970).
44. <http://www.casaxps.com>
45. B. S. Norgren, M. A. J. Somers, and J. H. W. Dewit, *Surf Interface Anal*, **21**, 378 (1994).

46. M. C. Biesinger, C. Brown, J. R. Mycroft, R. D. Davidson, and N. S. McIntyre, *Surf Interface Anal*, **36**, 1550 (2004).
47. A. P. Grosvenor, M. C. Biesinger, R. S. Smart, and N. S. McIntyre, *Surf Sci*, **600**, 1771 (2006).
48. A. M. Sukhotin, M. N. Shlepakov, and V. I. Popov, *Soviet Electrochemistry*, **21**, 1582 (1985).
49. D. D. Macdonald, *Pure Appl Chem*, **71**, 951 (1999).
50. HASTELLOY, *C-22 Alloy Product Brochure*, Haynes International Inc., <http://www.haynesintl.com/pdf/h2019.pdf>.